Performance enhancement of near-field thermoradiative devices using hyperbolic metamaterials

Alok Ghanekar, Yanpei Tian, Xiaojie Liu, Yi Zheng
Department of Mechanical, Industrial and Systems Engineering, University of Rhode Island, Kingston, RI 02881

Abstract. In this theoretical work, we analyze a near-field thermoradiative device that consists of an indium arsenide (InAs) based photodiode under negative illumination. We analyse a possible enhancement of conversion efficiency by use of hyperbolic metamaterial (HMM) in place of bulk metallic heat sink. A stack of alternating thin-films of metal (zirconium carbide (ZrC)) and dielectric (silicon dioxide (SiO_2)) is chosen to be the HMM under investigation. We analyze role of hyperbolic modes in near-field radiative transfer to enhance the energy conversion of the proposed device.

Keywords: thermoradiative device, near-field thermal radiation, hyperbolic metamaterials, photovoltaics.

*Yi Zheng, zheng@uri.edu

1 Introduction

Photovoltaic (PV) cells can be used to convert heat into electricity, the most commonly discussed configuration being a thermophotovoltaic (TPV) system.[1,2] A TPV system has a thermal emitter at high temperature that illuminates a PV cell which converts incident photons into electricity. In an alternative configuration, thermoradiative (TR) devices use PV cell at a higher temperature that lose heat to ambient or a heat sink.[3] This configuration also generates useful work and is considered as a PV cell under negative illumination. A PV cell can also be used in two more configurations for thermoradative energy conversion; namely, electroluminescent refrigerator and thermophotonic heat pump.[4] The concept of a TR device was first proposed by Byrnes et al.[5] in which it was suggested to use a rectifying antenna instead of a PV cell. This was extended to PV cell based TR device in a far-field configuration by Strandberg[3] and later validated experimentally by Santhanam and Fan.[6] When a PV is at a higher temperature than the ambient, it emits more photons than it absorbs. If this radiative transfer is restricted to interband transition in the bandgap, the number of free carriers (electrons and holes) is reduced and quasi-Fermi levels of these carriers are shifted.

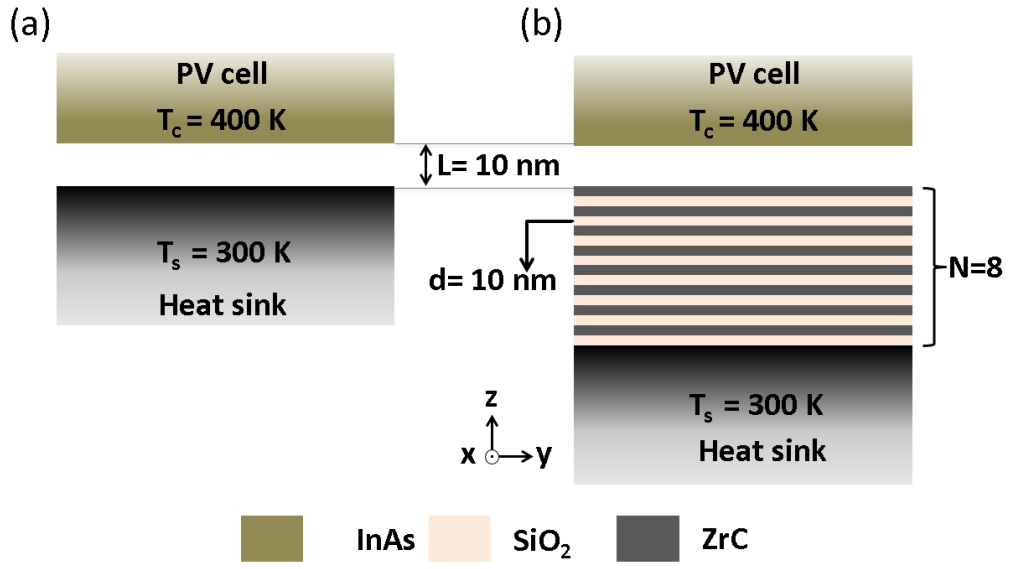

Fig 1 Schematic of a near-field thermoradiative device with (a) InAs based PV cell and bulk ZrC. (b) ZrC is replaced by a HMM of thickness 160 nm over bulk ZrC. HMM has alternative layers of ZrC and SiO_2.

This corresponds to a negative open circuit voltage. When short-circuited, this generates an electric current. A more detailed description of physical mechanism can be found in Strandberg.[3] A comparison between workings of TR and other PV based energy conversion systems can be found in Lin et al.[7]

In this work, we focus on a near-field TR cell that has a InAs based PV cell and a heat sink separated by a gap L much smaller than the wavelength of thermal radiation λ_{th}. In a near-field TR cell, the exchange of photons between PV cell and the heat sink is dominated by evanescent modes and surface modes of the materials involved. Maximum radiative exchange is possible when the plasma frequency of the heat sink is just above the bandgap frequency of the PV cell.[8,9] However, most metals have much higher plasma frequencies than the bandgap of common PV cells.[10] Wang et al.[9] showed that the power density of a TR cell can be significantly increased by using a 1-D grating structure that allows additional surface modes that can couple across the interfaces. In this paper, we show that additional channels of radiative heat transfer can also be created using a

metamaterial that supports hyperbolic modes. This leads to an enhanced power output of the TR cell.

A typical TR device is shown in Fig. 1(a). The photovoltaic cell and the heat sink are separated by a distance much shorter than the characteristic thermal wavelength. In the present study, it is assumed to be 10 nm. PV cell is InAs based with a bandgap of 0.3 eV. In the simplest configuration, heat sink is made up of bulk ZrC. We investigate possible enhancement of performance by using a HMM in place of bulk ZrC (Fig. 1(b)). In this case, ZrC is replaced by a HMM over a bulk ZrC substrate. The HMM has alternating layers of ZrC and SiO_2, each having thickness 10 nm. 8 Such layers of each ZrC and SiO_2 form a 160 nm thick HMM.

2 Theoretical formulations

Consider an ideal InAs based PV cell with the bandgap of 0.3 eV in which only radiative recombination process is responsible for losing electron-hole pairs. The cell temperature is T_c and sink temperature is T_s and they are separated by distance $L << \lambda_{th}$. Under non-equilibrium condition ($T_c \neq T_s$), if the splitting of quasi-Fermi levels of electrons and holes is μ, the PV cells emits according to the generalized Bose-Einstein distribution

$$\Theta(\omega, T, \mu) = \begin{cases} \dfrac{1}{e^{(\hbar\omega-\mu)/(k_B T_c)} - 1}, & \omega \geq \omega_g. \\ \dfrac{1}{e^{\hbar\omega/(k_B T_c)} - 1}, & \omega < \omega_g, \end{cases} \tag{1}$$

where ω is the frequency, ω_g is the bandgap frequency, $\hbar$ is the Planck's constant and k_B is the Boltzmann's constant. The generated current density from a TR cell under non-equilibrium condi-

tion is given by,

$$I(\mu) = e \int_{\omega_g}^{\infty} \frac{d\omega}{2\pi} T_{c\to s}(\omega, L)[\Theta(\omega, T_s, 0) - \Theta(\omega, T_c, \mu)], \tag{2}$$

where e is the elementary charge and $T_{c\to s}(\omega, L)$ is the transmissivity across the two interfaces as function of separation L. $T_{c\to s}(\omega, L)$ is energy transmission coefficient across the interfaces integrated over all wavevector components, i.e.

$$T_{c\to s(\omega)} = \int_0^{\infty} \frac{k_\rho dk_\rho}{2\pi} \xi(\omega, k_\rho). \tag{3}$$

The expression for energy transmission coefficient $\xi(\omega, k_\rho)$ for frequency ω and parallel wave vector k_ρ can be found elsewhere. Here the photodiode (PV) cell is under a reverse bias and therefore the associated voltage $V = \mu/e$ is negative and $I(\mu)$ are negative. This voltage can be varied by changing the load. The output power density to the applied load is given by,

$$P_{out} = VI(\mu). \tag{4}$$

The net radiative heat transfer between the cell and the sink is given by,

$$Q_{c\to s} = \int_0^{\infty} \frac{d\omega}{2\pi} \hbar\omega T_{c\to s}(\omega)[\Theta(\omega, T_s, 0) - \Theta(\omega, T_c, \mu)]. \tag{5}$$

As the cell is losing heat, $Q_{c\to s}$ is negative and the efficiency of the TR cell is given by $\eta = P_{out}/(P_{out} - Q_{c\to s})$.

Dielectric function of InAs is modeled using interband transition as in Adachi[11] and Aspnes

and Studna.[12] Using this model transmissivity across InAs cell and the sink is zero for $\omega < \omega_g$. Therefore, we only concern ourselves with frequency above the bandgap frequency. A stack of alternating layer of ZrC (metal) and SiO_2 (dielectric) can be seen as a homogeneous anisotropic uniaxial metamaterial with its optical axis (z) perpendicular to the layers using effective medium theory (EMT). Its dielectric function in ordinary mode $\varepsilon_\perp$ and extraordinary mode $\varepsilon_\parallel$ is given by[13]

$$\varepsilon_\perp = f\varepsilon_{ZrC} + (1-f)\varepsilon_{SiO_2} \tag{6a}$$

$$\varepsilon_\parallel = \frac{f}{f/\varepsilon_{ZrC} + (1-f)/\varepsilon_{SiO_2}}. \tag{6b}$$

ε_{SiO_2} and ε_{ZrC} are dielectric functions of SiO_2 and ZrC, respectively and can be found in literature.[14,15] As both layers have equal thicknesses, filling factor $f = 0.5$ in our case. This metamaterial is said to be hyperbolic for the frequencies where $\varepsilon_\perp \varepsilon_\parallel < 0$.[16,17] Using Eq. 6a and 6b, we found that for $1 < \omega/\omega_g < 1.609$, $\varepsilon_\perp < 0$ while $\varepsilon_\parallel > 0$, meaning the material is type II hyperbolic.[18] This means plasmonic motion is free along x and y direction, but it is restricted along z direction. For $1.609 < \omega/\omega_g < 2.831$, $\varepsilon_\perp > 0$ and $\varepsilon_\parallel < 0$ suggesting hype I hyperbolic behaviour.[18] For these frequencies, plasmonic oscillations are restricted in x and y directions but are free in z direction. Note that, EMT is used only to verify hyperbolic nature of the media. For calculations, exact multi-layer geometry with properties of ZrC and SiO_2 are used. EMT is applicable when the wavelength of interest is much larger than the period of the alternating layers. Minimum wavelength considered here is around 826 nm corresponding to $5\omega_g$ and it is much longer than the period of 20 nm in our case.

Figure 2 (a) shows the transmissivity across the TR cell for the two cases shown in Fig. 1. For bulk ZrC, the curve shows a resonance around $\omega/\omega_g \approx 2$. This corresponds to surface plasmon po-

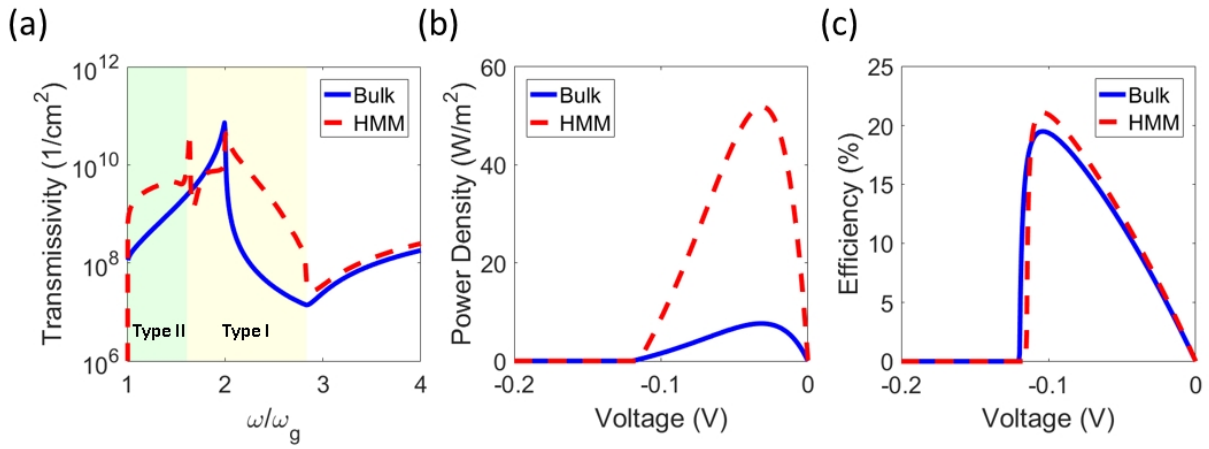

Fig 2 (a) Comparison of transmissivity across the TR cell, (b) output power density and (c) efficiency for the two cases investigated.

laritons of ZrC. As plasma frequency ω_p of ZrC is 1.29×10^{15} rad/s, frequency of surface plasmon resonance ω_{SPP} is $\omega_p/\sqrt{2} = 9.1 \times 10^{14}$ rad/s $\approx 2\omega_g$. Therefore, transmissivity between InAs and bulk ZrC displays resonance peak around that frequencies. Transmissivity for the configuration with the HMM heat sink clearly covers a broader frequency range when compared to that with bulk ZrC heat sink suggesting additional channels of heat transfer being available. Figure 2(a) and (b) plot power output density and TR cell efficiency against voltage for $T_c = 400$ K and $T_s = 300$ K. A trade off between power and efficiency is observed as peak power and peak efficiency occur at different voltages and it is typical of a TR cell. The HMM based TR cell shows a greatly increased power density but efficiency curve shows only a minor improvement. Increased transmissivity in the region closer to ω_g is responsible for increased power of HMM based TR cell. As seen in Fig. 2(b), the maximum power output density is increased nearly 7 times. Although the increase in efficiency is minor, we note that power density at the peak efficiency point ($\approx$ -0.1 V) has increased 5 times with the new heat sink. This means, more power can be produced at the same operating temperature. To further investigate increased power density, we plot the energy transmission coefficient for transverse magnetic (TM) polarization $\xi(\omega, k_\rho)_{TM}$ across the interfaces in $\omega/\omega_g : k_\rho c/\omega$

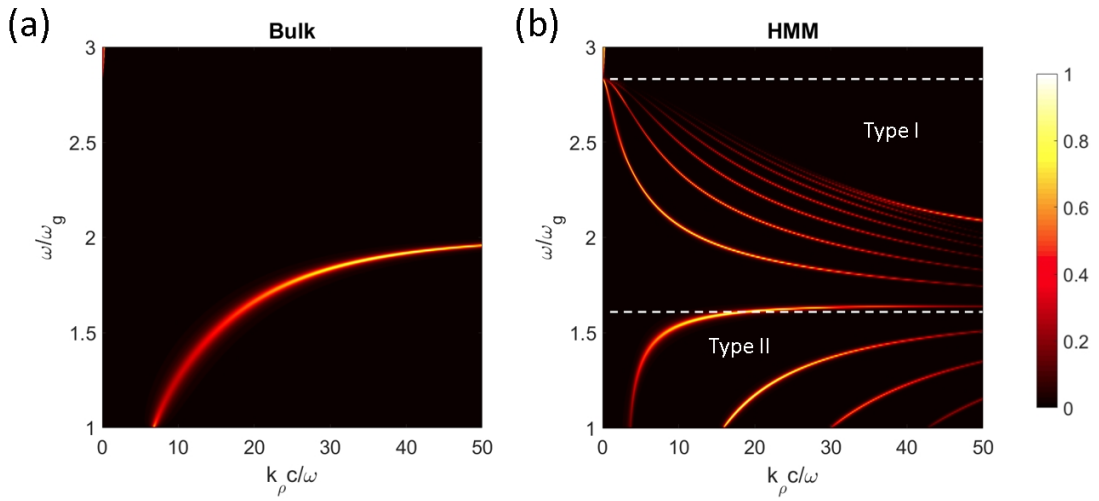

Fig 3 Coefficient of energy transmission for TM polarization $\xi(\omega, k_\rho)_{TM}$ across the near-field thermoradiative device under investigation when (a) the heat sink is bulk ZrC and (b) the heat sink is HMM.

space. Here, $k_\rho c/\omega$ represents normalized parallel wave vector with c being the speed of light. While Fig. 3(a) corresponds to a TR cell with bulk ZrC, Fig. 3(b) plot $\xi(\omega, k_\rho)_{TM}$ for the TR cell with HMM sink. With bulk ZrC as heat sink, typical dispersion relation associated with surface plasmon resonance is observed in Fig. 3(a). When bulk ZrC is replaced by a HMM layer, additional bands where surface resonance occurs are seen in both Fig. 3(b). These new resonances are coupled surface plasmon polaritons of ZrC layers that couple via SiO_2 layers. Additional hyperbolic modes at new frequencies are responsible for increased transmissivity across the interfaces, leading to increased power density. Fundamental difference between surface plasmon modes and hyperbolic mode is that surface plasmons exhibit evanescent field on the vacuum side as well as the material side while for the hyperbolic modes are propagating on the material side. Coupling of surface plasmons across the ZrC layers separated by SiO_2 allow this propagation.

Thus, we have demonstrated an improved performance of near-field theroradiative device upon use of HMM as heat sink. The power output of the TR cell relies upon coupling of surface modes at frequencies closer to the bandgap frequency of the PV cell. Hyperbolic metamaterial based heat

sink supports additional hyperbolic surface modes that lead to an increased radiative exchange of photons in the region closer to bandgap. A 7-fold increase in the output power density is observed without compromising the overall system efficiency. Presence of hyperbolic surface modes formed through coupling of surface modes of ZrC via SiO_2 layers is attributed to broadened transmissivity across the spectrum. As most metals have plasma frequencies higher than the bandgap of a typical PV cell, use of hyperbolic metamaterial as heat sink is one of the ways to reduce this mismatch.

Acknowledgments

This project was supported in part by a National Science Foundation through grant number 1655221, Institutional Development Award (IDeA) Network for Biomedical Research Excellence from the National Institute of General Medical Sciences of the National Institutes of Health under grant number P20GM103430, and National Aeronautics and Space Administration through grant number NNX15AK52A.

References

1 S. Basu, Y. Chen, and Z. Zhang, "Microscale radiation in thermophotovoltaic devices-a review," *International Journal of Energy Research* **31**(6), 689–716 (2007).

2 M. Bosi, C. Ferrari, F. Melino, *et al.*, "Thermophotovoltaic generation: a state of the art review," *Proceedings ECOS* (2012).

3 R. Strandberg, "Theoretical efficiency limits for thermoradiative energy conversion," *Journal of Applied Physics* **117**(5), 055105 (2015).

4 E. Tervo, E. Bagherisereshki, and Z. Zhang, "Near-field radiative thermoelectric energy converters: a review," *Frontiers in Energy* , 1–17 (2018).

5 S. J. Byrnes, R. Blanchard, and F. Capasso, "Harvesting renewable energy from earths mid-infrared emissions," *Proceedings of the National Academy of Sciences* , 201402036 (2014).

6 P. Santhanam and S. Fan, "Thermal-to-electrical energy conversion by diodes under negative illumination," *Physical Review B* **93**(16), 161410 (2016).

7 C. Lin, B. Wang, K. H. Teo, *et al.*, "A coherent description of thermal radiative devices and its application on the near-field negative electroluminescent cooling," *Energy* **147**, 177–186 (2018).

8 W.-C. Hsu, J. K. Tong, B. Liao, *et al.*, "Entropic and near-field improvements of thermoradiative cells," *Scientific reports* **6**, 34837 (2016).

9 B. Wang, C. Lin, K. H. Teo, *et al.*, "Thermoradiative device enhanced by near-field coupled structures," *Journal of Quantitative Spectroscopy and Radiative Transfer* **196**, 10–16 (2017).

10 P. B. Johnson and R.-W. Christy, "Optical constants of the noble metals," *Physical Review B* **6**(12), 4370 (1972).

11 D. E. Aspnes and A. Studna, "Dielectric functions and optical parameters of si, ge, gap, gaas, gasb, inp, inas, and insb from 1.5 to 6.0 ev," *Physical review B* **27**(2), 985 (1983).

12 S. Adachi, "Model dielectric constants of gap, gaas, gasb, inp, inas, and insb," *Physical review B* **35**(14), 7454 (1987).

13 P. Yeh, *Optical waves in layered media*, vol. 61, Wiley-Interscience (2005).

14 L. Gao, F. Lemarchand, and M. Lequime, "Refractive index determination of sio2 layer in the uv/vis/nir range: spectrophotometric reverse engineering on single and bi-layer designs," *Journal of the European Optical Society-Rapid publications* **8** (2013).

15 F. Modine, T. Haywood, and C. Allison, "Optical and electrical properties of single-crystalline zirconium carbide," *Physical Review B* **32**(12), 7743 (1985).

16 L. Hu and S. Chui, "Characteristics of electromagnetic wave propagation in uniaxially anisotropic left-handed materials," *Physical Review B* **66**(8), 085108 (2002).

17 D. Smith and D. Schurig, "Electromagnetic wave propagation in media with indefinite permittivity and permeability tensors," *Physical Review Letters* **90**(7), 077405 (2003).

18 Z. Jacob, "Quantum plasmonics," *Mrs Bulletin* **37**(8), 761–767 (2012).